A Miniature Pan-Tilt Actuator: The Spherical Pointing Motor

Benjamin B. Bederson, *Member, IEEE,* Richard S. Wallace, and Eric L. Schwartz, *Member, IEEE*

***Abstract*—A pan-tilt mechanism is a computer-controlled actuator designed to point an object such as a camera sensor. For applications in active vision, a pan-tilt mechanism should be accurate, fast, small, inexpensive and have low power requirements. We have designed and constructed a new type of actuator meeting these requirements, which incorporates both pan and tilt into a single, two-degree-of-freedom device. The spherical pointing motor (SPM)[1] consists of three orthogonal motor windings in a permanent magnetic field, configured to move a small camera mounted on a gimbal. It is an absolute positioning device and is run open-loop. The SPM is capable of panning and tilting a load of 15 grams, for example a CCD image sensor, at rotational velocities of several hundred degrees per second with a repeatability of .15°. We have also built a miniature camera consisting of a single CCD sensor chip and miniature lens assembly that fits on the rotor of this motor. In this paper, we discuss the theory of the SPM, which includes its basic electromagnetic principles, and derive the relationship between applied currents and resultant motor position. We present an automatic calibration procedure and discuss open- and closed-loop control strategies. Finally, we present the physical characteristics and results of our prototype.**

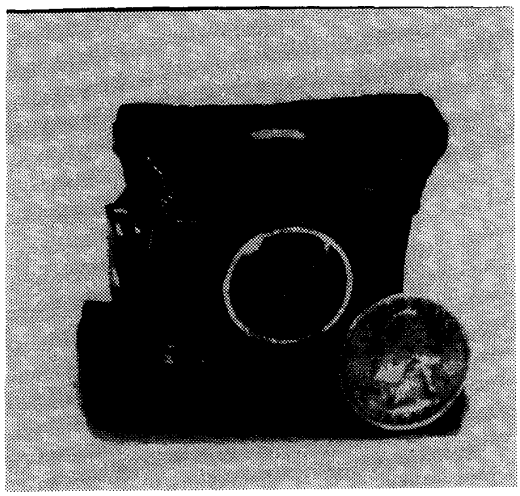

Fig. 1. The spherical pointing motor. At the center is a miniature camera consisting of a single CCD sensor chip and a lens assembly that fits on the rotor.

I. Introduction

A PAN-TILT mechanism is a computer-controlled actuator designed to point an object such as a camera sensor. For applications in active vision, it is desirable for a pan-tilt mechanism to be accurate, fast, small, inexpensive and to have low power requirements. We have constructed a new type of actuator meeting these requirements. It incorporates both pan and tilt into a single two degree of freedom device (Fig. 1). The spherical pointing motor (SPM) consists of three orthogonal motor windings in a permanent magnetic field, configured to move a small camera mounted on a gimbal. It is an absolute positioning device and is run open-loop.

The simplest and most obvious pan-tilt mechanism is the two-stage motor-on-motor (MOM) design. The first motor turns the mechanism through one degree of freedom (DOF), usually pan, and the second through the other DOF, usually tilt. The second motor must be powerful enough to move the camera sensor. The first must move both the camera and the second motor. The MOM design therefore usually consists of one larger motor and one smaller one. Such a design is inefficient because, as we show, it is not necessary to carry one motor on top of another one. An example of a commercially available MOM design is the pan-tilt actuator shown in (Fig. 2).

An alternative to the inefficiencies of the MOM design uses a parallel linkage. We experimented with this approach with the Platform Pantilt, a pan-tilt actuator based on two linear stepper motors (Fig. 3).

The Platform Pantilt moves a platform by raising and lowering two shafts with linear stepper motors that, along with a third fixed shaft, are attached to the platform. The shafts are fixed to single and double universal joints, as shown in Fig. 3. This design is similar in some respects to the six-degree-of-freedom Stewart platform [14], [24], [25]. The Platform Pantilt measures 7.5 × 7.5 × 12 cm and can move at rotational velocities of up to 100°/sec. The precision is somewhat limited, however, due to the use of stepper motors, and it is difficult to build this device in a small scale.

To overcome the limitations of the linkage approach, we implemented the spherical pointing motor (Fig. 1), a single direct drive motor with two degrees of freedom. The SPM is capable of panning and tilting a load of 15 gm, for example a CCD image sensor, at rotational velocities of up to 600°/sec. We have also built a miniature camera consisting of a single

Manuscript received April 14, 1992; revised July 26, 1993. This work was supported in part by DARPA/ONR Contract #N00014-90-C-0049, and AFOSR Contract #88-0275.

Benjamin B. Bederson is with Bell Communications Research, Morristown, NJ, USA.

Richard S. Wallace is with New York University, Courant Institute of Mathematical Science, New York, NY, USA.

Eric L. Schwartz is with Boston University, Cognitive Neural Systems, Boston, MA, USA.

IEEE Log Number 9215091.

[1] The spherical pointing motor is protected by U.S. Patent #5,204,573.

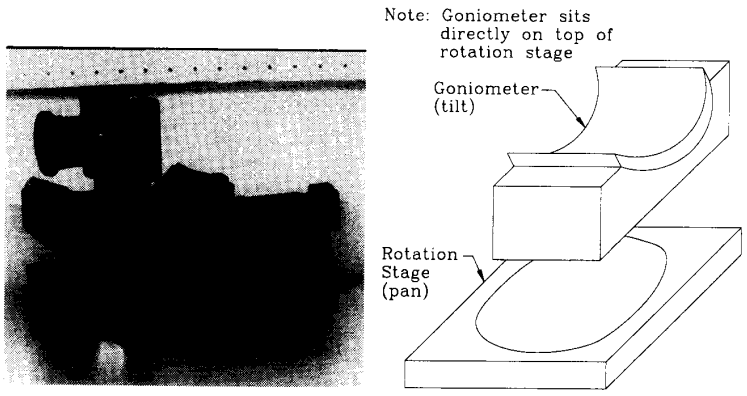

Fig. 2. Photo and illustration of a conventional motor-on-motor design. Actuator from Klinger Scientific.

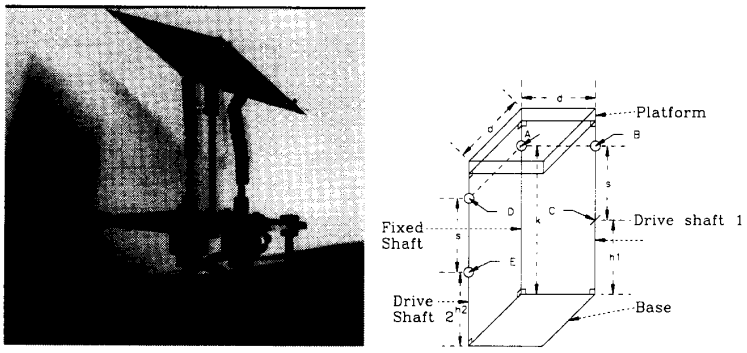

Fig. 3. The platform pantilt. Photo (left). This stepper motor-based actuator is capable of positioning a load of 80 grams; for example a small video camera. Illustration (right). The three dimensional mechanism we use. Note that circles at points A, B, D and E denote universal joints with two degrees of freedom while the line at point C denotes a pin joint with only one degree of freedom.

CCD sensor chip and lens assembly that fits on the rotor of this motor. The complete camera head is $8 \times 8 \times 10$ mm and weighs 6 gm. The prototype SPM is $4 \times 5 \times 6$ cm and weighs 160 gm. The SPM is part of a space-variant active vision system described in [4], [6], and [27].

II. Background

Pan-tilt mechanisms have been a source of inspiration and frustration to computer vision researchers. The source of inspiration is nature, where humans and animals rely on eye movements to achieve wide field-of-view visual sensing. But the argument from nature is not by itself a compelling reason to build robot eyes that pan and tilt. The alternative to mechanical pan-tilt action is electronic scanning; i.e., computer control of a fixed set of cameras having a combined wide field-of-view. Selective attention can be implemented by a variety of addressing methods; for example, the inverted pyramid of Burt [7], [8]. Such "software pan-tilt" mechanisms are considerably more convenient and reliable than their motorized counterparts. At present, the relative advantages of software- versus hardware-based active vision is an unresolved problem, and many research groups are pursuing both strategies.

One source of frustration with pan-tilt devices is acquiring or building, then calibrating and controlling the mechanism itself. Until recently, no manufactures have provided devices specifically designed for computer control of robot cameras. Low-speed inexpensive motorized pan-tilt camera platforms are available, for example from Edmund Scientific (catalog number F38,485), but these have no computer controls. Remote control pan-tilt devices intended for security camera applications, for example the Graystone Model V370PT, tend to be too slow (6 degrees per second) and too heavy (16 lbs.) for many robotic applications. Few of these devices have computer controls or position feedback information other than visual. The motion picture industry has also developed computer controlled pan-tilt devices. One example is the Kaleidoscope Hothead II, made by Shepperton Film Studios. Although a digital interface is available, this device is intended to carry a large load, such as a 35 mm motion picture camera, and although it achieves relatively high speed (140°/sec), it is very expensive. Another source of pan-tilt mechanisms is the lighting industry, which applies them to stage lighting, exhibition, and advertising. A high-speed computer controlled pan-tilt mechanism for stage lights is available from Multiline, but its bracketing and high cost make it unappealing for robot vision. A number of manufacturers (for example

Aerotech, Daedel, Unislide, and Klinger Scientific) make computer controlled mechanisms that can be assembled into pan-tilt devices. Better suited for manufacturing and optics applications, the high resolution of these devices (less than 1 arc minute) makes them overqualified for many computer vision applications and contributes to their high cost and weight.

Perhaps because of their familiarity and availability, if not their generality and programmability, robot arms have often been the choice of vision researchers trying to actuate their cameras. Baloch and Waxman used a 5-axis robot arm mounted on top of a mobile robot as a camera pointing mechanism [3]. Allen also reported mounting a TV camera on a robot arm [2]. Raviv used a Cartesian manipulator to implement camera pan, tilt, roll, and translation [22].

A number of researchers have embarked on building their own pan-tilt devices by assembling existing actuators and linkages. Krotkov built what is now recognized as the first robot head, a computer controlled mechanism for moving two cameras [19]. Abbot and Ahuja report an 11-degree-of-freedom mechanism to control pan, tilt, vergence, horizontal translation, and lens parameters [1]. From Osaka University, Kawarabayashi *et al.* report building an active vision "head" to control pan, tilt, vergence, zoom, and focus parameters of a pair of cameras [17]. The pan-tilt mechanism in all three of these designs is a MOM design. Dickmanns also reports a "fast" two-axis pan-tilt device carrying two cameras, one with a wide-angle view and the other telephoto, mounted atop their robotic automobile [12]. At Harvard, Clark and Ferrier constructed a seven-degree-of-freedom "head" to control pan, tilt, and the vergence, focus, and aperture of two cameras [10]. At least one two-eye system, the Rochester Robot [9], contains independent pan controls for two cameras on a tilting platform, in contrast to other systems in which vergence is coupled [9].

Another line of research pursued by several groups, including ourselves, is in the design of new actuators capable of two or more degrees of freedom. Davey *et al.* [11] analyzed a theoretical spherical induction motor originally described by Williams, Laithwaite, and Eastham [20]. Lee and Kwan [21] performed the initial analysis of a theoretical three-degree-of-freedom actuator based on stepper motor technology. Foggia *et al.* [13] built a prototype three degree of freedom actuator based on induction motors, while Hollis, Salcudean, and Allan [16] built a very high resolution prototype six-degree-of-freedom actuator based on magnetic levitation, designed to be used as the end-effector on a coarse-motion device.

The principal thrust of the present paper is the control of two degrees of freedom (pan-tilt) with a single, direct-drive actuator, with sufficient speed and accuracy to provide a basis for light weight and inexpensive active vision systems.

III. Spherical Pointing Motor Theory

The spherical pointing motor (SPM) is an absolute positioning device, designed to orient a small camera sensor in two degrees of rotational freedom. The basic principle is to orient a permanent magnet to the magnetic field induced by three

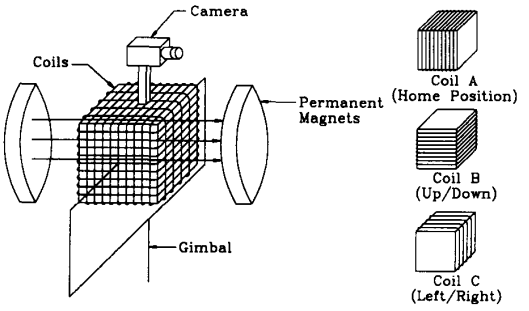

Fig. 4. (left) Illustration of the internal spherical pointing motor shown in its home position. (right) Labels for the three coils.

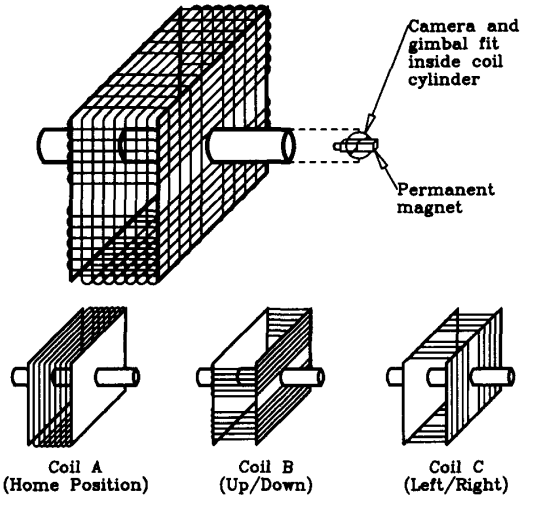

Fig. 5. (top) Illustration of the external spherical pointing motor shown in its home position. (bottom) Labels for the three coils.

othogonal motor windings by applying the appropriate ratio of currents to the three coils. A simple way to understand this device follows: The net magnetic field of the three coils may be visualized as defining a vector (dipole) oriented at angles (Θ, Φ) on the unit sphere. The angles (Θ, Φ) are determined by the three coil currents. The rotor dipole then aligns itself with the net coil field to provide the actuation.

We have built two types of SPM's: one having the coils on the inside, free to rotate on a gimbal inside a fixed magnetic field (Fig. 4); the other having the coils on the outside and the magnets attached to the gimbal inside the coils (Fig. 5). It is possible to build the smallest possible motor using the external coil design, so that is the approach we focus our attention on.

Both designs are constrained by two principles that affect the range of motion of the motor. The SPM is meant to be used as a pointing device. As such, it has a "home position," defined as the initial resting position from which the motor can make pan or tilt excursions of limited extent. Assuming that we want the home position to be centered within the possible excursions, we are led to the following constraints:

1) The permanent magnet must be positioned so that the field it defines is orthogonal to both axes of rotation of the gimbal when it is in home position.

2) The camera must be positioned on the rotor so that its optical axis is orthogonal to both axes of rotation of the gimbal when it is in home position. Note that this is equivalent to being aligned with the magnetic field if the first design constraint is satisfied.

These design principles arise because the motor is limited to two mechanical degrees of freedom and because the motor rotation can not be controlled about an axis aligned with the permanent magnetic field. To understand why this is so, we must examine the electromagnetic principle that provides the torque to move the motor.

The force on the coils comes from the basic electromagnetic principle that there is always an induced force on a current-carrying wire in a permanent magnetic field. Further, there will be a torque on a current-carrying wire loop in a permanent magnetic field in such a direction that the loop will move to make the normal to the plane of the loop align with the magnetic field.

Given a coil of wire in a uniform magnetic field $\mathbf{B}$, the torque τ exerted on the coil is the cross product

$$\tau = \mathbf{M} \times \mathbf{B} \tag{1}$$

where $\mathbf{M}$ is the magnetic dipole moment having direction perpendicular to the coil and magnitude

$$|\mathbf{M}| = NiA \tag{2}$$

where N is the number of windings in the coil, i is the current in the wire, and A is the area inside each winding [15], [18]. The sign of $\mathbf{M}$ is determined by the direction of current in the wire loop. When a nonzero current i flows through the loop, there will be a torque on the loop so that the loop will rotate to its minimum energy configuration where $\tau = 0$; i.e., $\mathbf{M}$ is aligned with $\mathbf{B}$.

By (1), the torque is maximum when the angle between $\mathbf{M}$ and $\mathbf{B}, \Theta = 90^\circ$ and drops to nothing when $\Theta = 0^\circ$. This angle is the angular distance between the motor's current position and its destination position. When the coil is at position $\Theta = 0$, it is at its minimum potential energy and there is no force on it. Because of this relationship between torque and angle, the friction of the bearings must be minimized. The precision of the motor is inversely related to the amount of friction in the bearings. This is because fine movements of the motor occur at very small angles where the torque is very small, and such fine movements must overcome the friction of the bearings.

We now examine the first design constraint. If this constraint is not satisfied, then it is not possible to both pan and tilt the motor from the home position. Coils A and B control the tilting, while coils A and C control the panning (Fig. 4). When the motor has panned 90°, coil B has kept its original orientation with respect to the magnets, but coils A and C have swapped their relative orientation. This is depicted in Fig. 6 for the internal coil motor and the analog for the external coil motor is in Fig. 7. This position can be reached by energizing coil C while turning off coils A and B. In this position, the pan angle is controlled, but there is no way to control the tilt angle in this orientation. This is because the tilt axis is aligned with the magnetic field and no torque can be exerted around this axis. This is proved in Section IV. Without the first design constraint, the home position could be as depicted in Fig. 6, in which case the motor could not be tilted along the vertical meridian.

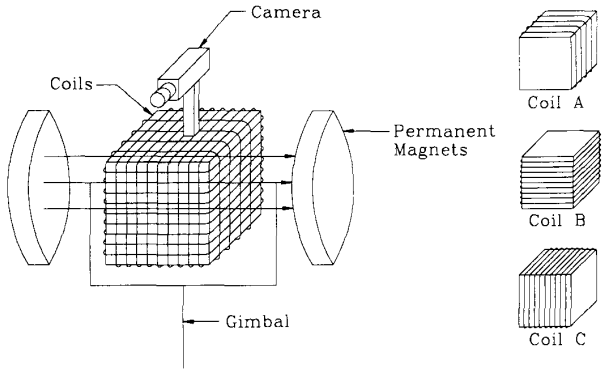

Fig. 6. (left) The internal coil motor panned 90° so that tilting is not possible. (right) The coil labels for the motor in this position. Notice how coils A and C have swapped orientations.

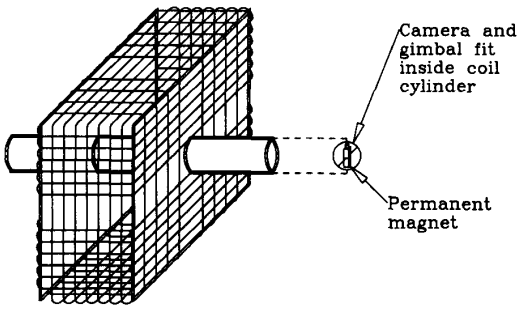

Fig. 7. The external coil motor panned 90° so that tilting is not possible.

The second design constraint stems from assuming that the two degrees of freedom desired for the camera are pan and tilt. If instead, roll (rotation about the optical axis) and either pan or tilt is desired, then the second design constraint is not necessary. This constraint comes directly from the mechanical degrees of freedom available. If pan and tilt are desired, the camera's optical axis must be orthogonal to the two degrees of mechanical freedom.

This has an undesirable affect for the internal coil motor. Because the first design constraint requires that the permanent magnets must also be positioned orthogonally to both axes of rotation, the optical axis of the camera must be aligned with the permanent magnetic field. Since the camera is between the two permanent magnets, its field of view will be obscured by the magnets. Therefore, some method of looking over the magnets must be found. This could possibly be done with mirrors, or as depicted in Figs. 5 and 7, the camera could be mounted on a stalk. This gives the external coil motor a clear advantage because the camera is located in the center of the motor. This not only decreases the moment of inertia, but also allows the camera to be rotated around the focal point of the lens, which is usually desired for machine vision applications.

IV. Theoretical Calculation of Motor Position

Here we investigate the relation between motor orientation and coil currents. The current in each coil induces a magnetic field normal to the plane of the coil. Because the magnetic fields from the three coils add vectorially, only the ratio of the currents through the coils is important to determine orientation. The motor is an absolute positioning device. This means that applying a set of currents to the coils creates a torque on the rotor that will turn it to the position of lowest potential energy. At this point, there is no torque, and thus no movement. In this section, we assume ideal coils; i.e., they are perfectly symmetrical, have the same number of turns, and are the same size. We deal with the realistic case by calibrating the motor in Section V.

A. Position Given Currents

From (1), we know that the torque on a coil is proportional to the sine of the angle between the normal to the coil and the magnetic field. If $\mathbf{M}$ is aligned with $\mathbf{B}$, pointing in either the same or the opposite direction, there is no torque. However, when they are pointing in the same direction, the potential energy is minimum and the coil is in a stable resting state. If they are pointing in opposite directions, the potential energy is maximum and the coil is in an unstable resting state. If the coil is slightly perturbed, it will swing around 180° to reach the minimum potential energy state.

We will use the external coil motor as an example, but the following derivation applies equally to the internal coil motor. Here we talk about torque on the magnets for the external coil motor, but an equal torque acts on the coils for the internal coil motor. For example, the torque on the magnets due to coil A for the external coil motor is equivalent to the torque on coil A for the internal coil motor.

We will use the coil labels shown in Fig. 4. As the torque from each coil is dependent on the motor orientation, we must calculate when the sum of the torques on all three coils vanishes. The resting position is determined by

$$\tau_{\mathrm{A}} + \tau_{\mathrm{B}} + \tau_{\mathrm{C}} = 0. \tag{3}$$

We define the coordinate system we will use in Fig. 8. Here, both the permanent magnetic field and the home position are defined to lie in the direction of the positive x-axis. Θ (or tilt angle) is defined as the positive rotation about the z-axis and Φ (or pan angle) is defined as the negative rotation about the y-axis.

Let us examine the torque due to coil A. The magnetic field, $\mathbf{B} = (1, 0, 0)$. When the motor is in home position, coil A has the magnetic dipole moment, $\mathbf{M}_A = N_{\mathrm{A}} A_{\mathrm{A}} i_{\mathrm{A}} (1, 0, 0)$. We use the constant $K_A = N_A A_A$. To calculate the torque from coil A at position (Θ, Φ), we rotate $\mathbf{M}_{\mathrm{A}}$ by Θ around the z-axis and then by Θ around the y-axis, yielding the new dipole moment, $\mathbf{M}'$.

$$\begin{aligned}\mathbf{M}'_A &= K_{\mathrm{A}} i_{\mathrm{A}} (1, 0, 0) \cdot [\mathrm{rot}_Z(\Theta)] \cdot [\mathrm{rot}_Y(\Phi)] \\ &= K_{\mathrm{A}} i_{\mathrm{A}} (\cos\Theta \cos\Phi, \sin\Theta, -\cos\Theta \sin\Phi)\end{aligned}$$

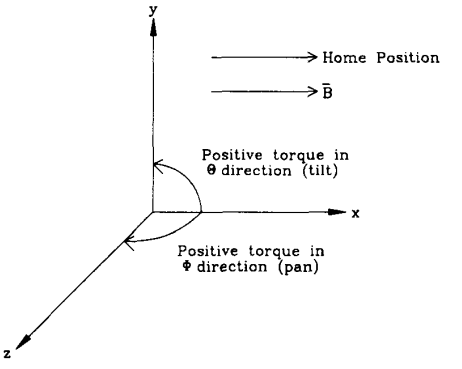

Fig. 8. The coordinate system used for calculations. The permanent magnetic field and the home position both lie along and in the direction of the positive x-axis.

Then,

$$\begin{aligned}\tau_A &= \mathbf{M}'_{\mathrm{A}} \times \mathbf{B} \\ &= K_{\mathrm{A}} i_{\mathrm{A}} (0, -\cos\Theta \sin\Phi, -\sin\Theta)\end{aligned}$$

We can calculate the torque from coils B and C similarly. Finally, we calculate the position using (3).

$$\begin{aligned}&K_{\mathrm{A}} i_{\mathrm{A}} (0, -\cos\Theta \sin\Phi, -\sin\Theta) \\ &\quad + K_{\mathrm{B}} i_{\mathrm{B}} (0, \sin\Theta \sin\Phi, -\cos\Theta) \\ &\quad + K_{\mathrm{C}} i_{\mathrm{C}} (0, \cos\Phi, 0) = 0\end{aligned}$$

This results in the solution

$$\Theta = \tan^{-1}\left(\frac{-K_{\mathrm{B}} i_{\mathrm{B}}}{K_{\mathrm{A}} i_{\mathrm{A}}}\right) \tag{4}$$

$$\Phi = \tan^{-1}\left(\frac{K_{\mathrm{C}} i_{\mathrm{C}}}{K_{\mathrm{B}} i_{\mathrm{B}} \sin\Theta - K_{\mathrm{A}} i_{\mathrm{A}} \cos\Theta}\right) \tag{5}$$

Thus, the position of the motor (Θ, Φ) can be calculated given the currents applied to the three coils.

B. Current Given Position

Given a desired motor position, we would like to calculate the coil currents necessary to attain that position. As previously stated, because there are three coils and only two mechanical degrees of freedom, the motor position depends upon the ratio of the currents in the coils. Thus, we can fix one of the coil currents, and calculate the other relative currents. Then the scale of the three currents will control the torque with which the motor is moved to the specified position. Note that the three degrees of freedom corresponding to the three coil currents are (Θ, Φ), and magnitude of the torque, τ.

Assume i_{A} constant. Then from (4) and (5),

$$i_{\mathrm{B}} = \frac{-K_{\mathrm{A}}}{K_{\mathrm{B}}} i_{\mathrm{A}} \tan\Theta \tag{6}$$

$$i_{\mathrm{C}} = \frac{-K_{\mathrm{A}} i_{\mathrm{A}}}{K_{\mathrm{C}}} (\sin\Theta \tan\Theta + \cos\Theta) \tan\Phi \tag{7}$$

The three currents are then scaled so that the largest current magnitude is set to a maximum, $i_{\max}$. That is,

$$\max(|i_{\mathrm{A}}|, |i_{\mathrm{B}}|, |i_{\mathrm{C}}|) = i_{\max}$$

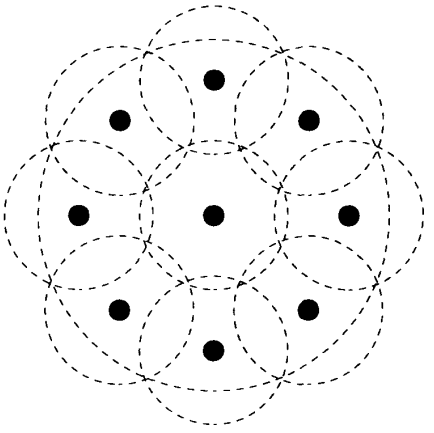

Fig. 9. The solid dots comprise the scene used to calibrate the SPM. The nine smaller dashed circles are not part of the calibration pattern, but represent the field of view of the camera when centered on each dot. The single large dashed circle is also not in the scene, but represents the workspace of the motor. The entire workspace of the motor is covered by the small dashed circles.

Fig. 9 shows plots of the calculated currents versus position for each of the three coils along with the actual currents produced from the calibration procedure described in Section V.

V. Calibration

The calculation of motor position for specified currents would be accurate in the ideal case where all three coils were perfectly symmetrical, had the same number of turns, and were the same size. In general, none of these things are true. Thus the calculated currents gives only an approximation to the actual position of the motor.

The motor must be calibrated to associate motor positions with the related set of currents that moves the motor to these positions. Only a small number of calibration points are necessary (depending on the desired precision of the motor). Points between the calibrated positions can be approximated with linear interpolation.

We have developed a procedure for automatic calibration of the SPM. It is based on image feedback from a camera mounted on the rotor of the motor. It assumes that a calibrated image sensor and lens are used; i.e., that it is known how many degrees each pixel subtends, and that this is constant throughout the field of view. The basic idea is that a scene of black dots on a white background is imaged. For each motor position that is to be calibrated, the motor is moved approximately to that position using the calculated currents of Section IV. The image is analyzed, and the position of the relevant dot is used to calculate the actual position of the motor. This position is then associated with the coil currents by creating a look-up-table that stores the three coil currents for each motor position.

The workspace of the motor is larger than the field of view of the camera, so the scene must consist of more than one dot. To make the calibration procedure as automatic and as easy to use as possible, we do not want to measure the scene externally. Instead, the algorithm should work with only

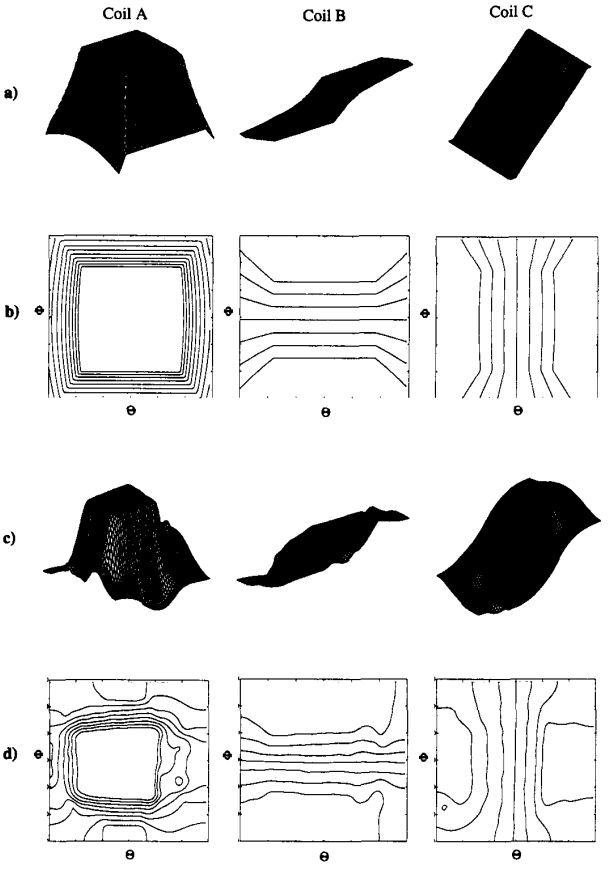

Fig. 10. (a) Theoretical currents versus position for each of the three coils shown as a mesh plot. (b) The same as (a) shown as a contour plot. (c) Calibrated currents versus position for each of the three coils shown as a mesh plot. (d) The same as (c) shown as a contour plot. The data shown here is for the $\pm 30°$ workspace in (Θ, Φ). For all the plots in this figure, $\{\Theta, \Phi \in [-30°, 30°]\}$.

approximate knowledge of the positions of the dots. The only requirement is that there are enough dots so that the entire workspace of the motor is covered, and that it is possible to view the dots in pairs so that the position of one dot can be determined by its position relative to that of a previously calibrated one. In this way, the position of each dot can be precisely measured automatically by the calibration procedure. The scene used to calibrate the prototype motor is shown in Fig. 10.

The algorithm assumes the scene is arranged so that initially the center dot is approximately centered in the motor workspace, and thus within the camera's field of view when the motor is in home position. Information about the arrangement of the scene is supplied to the algorithm.

In this algorithm, the dot is defined as a single connected component whose values are below a threshold that is assumed to have been previously computed. The prototype SPM has been calibrated using this technique with the scene depicted in Fig. 10. The results are shown in Fig. 9 along with the ideal case. The currents for each coil are shown over a workspace of $\pm 30°$ in Θ and Φ. See [5] for more details about the calibration of the SPM.

VI. Dynamics and Control

The dynamics of the spherical pointing motor are approximately that of a simple second order system. When a new set of currents are applied to the coils, a torque is created that moves the rotor to the new position. As calculated in Section IV, this torque is dependent on the angle between the current motor position and the destination position. Let us call this angle Ψ.

The motor will accelerate toward the destination position with the torque decreasing as it is reached. However, it will overshoot and ring around the final position. The ringing is described as follows. The torque $\tau = \kappa \sin \Psi$ for some κ. For small angles, $\sin \Psi \approx \Psi$. Then the position of the motor will follow (8) [15, p. 228].

$$-\kappa\Psi - b\frac{d\Psi}{dt} = I\frac{d^2\Psi}{dt^2} \tag{8}$$

where b is the damping constant and I is the rotational inertia of the rotor. The approximate solution to this is

$$\Psi \approx Ae^{-bt/2I}\cos(\omega t + \alpha) \tag{9}$$

where A and α are constants, and the exponential function describes the magnitude envelope of the ringing. The frequency of the ringing is $\omega \approx \sqrt{\kappa/I}$.

The ringing of the SPM was measured by recording the induced voltage of the ringing on a pickup coil of magnet wire that was placed adjacent to the SPM. Because the pickup coil measures the change in magnetic field, we measured velocity of the ringing. The recording was made by amplifying the induced voltage and digitizing this through the audio port of a Sun Sparcstation at a sample rate of 8 KHz (after filtering the signal with an FFT to isolate the ringing from the 1 KHz PWM noise). After the measurements were made, we found that the Sun input channel is AC-coupled, and effectively differentiated our signal; thus we actually recorded the acceleration of the ringing of the SPM. Because the actual ringing is very closely modeled by a damped sin function, and the second derivative of a sin is a sin, the acceleration of the ringing that we recorded is proportional to the ringing, and we used this measurement to judge the relative performance of our control techniques.

The ringing can be greatly reduced by various open-loop control methods. Perhaps the simplest strategy is to move the motor from the initial position to the destination position in small decreasing increments at fixed time intervals. This way, maximum motor velocity is traded off for control. Including the time it takes for ringing to stop, the controlled approach yields a faster average velocity. This method is implemented by moving a fixed percentage of the distance between the current position and final position at each step. This will decrease the motor movement with each step. The motor velocity can then be controlled with either the percentage movement of each step, or the time interval between steps. We use a constant time interval, and vary the percentage movement of each step to experiment with different speeds. We call this the *fixed percentage* control method.

A second slightly more complicated open-loop control strategy based on conventional stepper motor control theory yields better results [23]. The idea, which we call the *two step* method, is based on the fact that the SPM rotor oscillates with an approximately constant period. We first step the motor to a point midway between the initial and destination positions. This midpoint is determined from the calibration results of Section V. We then wait for the ringing velocity to be zero, at which point we apply a second step to hold the rotor at this position of zero velocity. The energy of the ringing will be largely dissipated, and the rotor will be at the destination position. Although, we don't know exactly when to apply the second step, we can estimate it by waiting half the period of oscillation. This assumes that the period of oscillation is constant, which is not true, but is a close approximation. In practice, because neither the midpoint nor the time at which the currents are changed are exactly correct, not all of the ringing energy is dissipated, and a little ringing of the same period remains—but with vastly reduced amplitude. This approach is unusual in that it takes a constant time to move any distance, where the time is half the period of oscillation. A sample result of this approach is shown in Fig. 11.

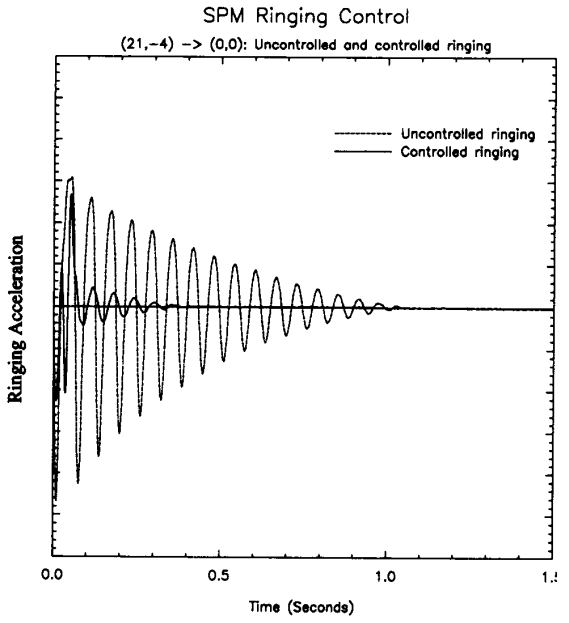

Fig. 11. Measurement of two-step open-loop control strategy to reduce SPM ringing. Results are shown for the same movement of 21° with and without control. The motor currents are changed to hold the motor at the final position when the motor is expected to have zero velocity. Because the midpoint and timing are not exactly correct, the ringing is not completely eliminated.

We attempted to compensate for the imprecision of the *two-step* strategy by various combinations of the previous two control strategies. The first approach is to apply the two-step method twice, first moving to the midpoint, and then to the destination point. This method theoretically also takes a constant time, which is twice as long as the single two-step method. We call this approach the *dual two-step* method.

A final variation, called the *multi two-step* method, is to apply the two-step method multiple times with logarithmically decreasing steps. The motor is always moved half way between its current position and the destination position with the two-

step method. This takes time $O(\log(\Psi))$ where Ψ is the total angular distance.

Results from these open-loop control strategies are presented in Section VII-B.

One of the motivating factors behind the development of the SPM was to make a motor that could be run by an open-loop controller, and we have accomplished this task. However, if higher performance is needed, a velocity or position sensor could be added to run the motor with a closed-loop control strategy. This would allow the two-step control strategy to be applied more accurately, as the zero-velocity point would be known exactly. Not only would this increase the speed of the motor, but it would also increase its accuracy. The motor's supply currents could be 90° out of phase with the position, as with conventional DC motors. This would result in always driving the motor at its maximum torque, and thus the torque would no longer be dependent on the difference between the current and destination position. Max and Wallace at New York University have continued development of SPM's and have implemented a closed-loop control method for them [28].

VII. Prototype Spherical Pointing Motor

The prototype SPM (Fig. 1) is $4 \times 5 \times 6$ cm, weighs 160 gm and is capable of actuating a 15 gram load. Its total workspace is approximately 60° in both the pan and tilt directions.

We measured the maximum torque of this motor with a digital force meter at a known moment arm, and found it to be $0.008Nm$ at $1.0A$. The torque constant, $K_\tau = \tau/i = 0.008Nm/A$. The motor constant, $K_m = K_\tau/\sqrt{R} = 0.0016Nm/\sqrt{W}$. This is within a factor of ten of similar sized commercially available brushless motors. Wallace [26] built a newer SPM prototype with a motor constant, $K_m = 0.02Nm/\sqrt{W}$.

A. Precision and Repeatability

The precision of the motor is defined as the angular distance between adjacent positions. If the controller consisted of an analog variable current source, the motor's precision would be infinite. As we are using a digital PWM controller, the precision with which we can control the motor is limited by the step size of the PWM duty cycle. The step size is dependent on the frequency of the PWM. Lower frequencies have more precise control of the step. However, lower frequencies also introduce a choppiness that vibrates the motor. We use a 1 KHz frequency and are able to specify 4000 steps in the duty cycle (i.e., 4000 different duty cycles). As the duty cycle of the PWM on a single coil with a specified polarity changes between 0 and 100, the motor will turn at most 45°. Thus, we can position the motor to steps no smaller than $45°/4000 = 0.011°$ or 0.68 minutes of arc.

The repeatability of the motor is dependent mostly on the friction of the bearings. As there is no iron core, there is no hysteresis. Because the motor is not perfectly balanced, the motor position is not constant at different orientations to gravity, but at a fixed orientation the accuracy is dependent only upon the friction of the bearings.

We measured the motor's repeatability with a laser setup and found the motor to be repeatable to .15°. The camera mounted in our motor returns 192×165 pixels with a 33.6° horizontal field of view. This is equivalent to .175° per pixel. For our camera and lens, the SPM is thus repeatable to about one pixel.

The repeatability of the SPM was measured by reflecting a laser diode off a reflective surface attached to the rotor, and measuring the position of the reflected beam on the wall several feet away. The motor is set at a fixed position with the rotor positioned at the place to be measured. The laser is then oriented so that the reflected beam hits the wall at a right angle. This point on the wall is recorded. The motor rotor is moved away and then back to the original position. The distance between the new reflected laser position and the original position is measured. The repeatability of the motor is then calculated in degrees as derived from the geometry of the setup.

B. Velocity Measurements

We measured the average velocity of the motor for point to point motions, since we have no ability to measure instantaneous velocity. We recorded the velocity using the technique described in Section VI for measuring the ringing. The motor controller was programmed to accept motion commands with a specified control strategy over an RS-232 serial port. A program running on a Sun Sparcstation controlled the SPM and automatically recorded and analyzed the results. For each control strategy, ten measurements were made at each of ten different angular movements. The averaged results with error bars showing the variance of each experiment are shown in Figs. 12, 13, and 14.

A summary of the control strategies measured follow:

1) *No control.* Base line for comparing control strategies.
2) *Fixed percentage.* The motor is moved a fixed percentage of the distance between its current position and the destination position with a fixed delay between each movement. By making the percentage of movement per step small enough, the ringing can be completely eliminated at the expense of decreased velocity. Results shown here are for a percentage selected such that a small amount of uncontrolled ringing remained at the end of the motion.
3) *Two-step.* The motor is moved to the midpoint between the initial and destination positions. After a delay equal to half the period of the natural motor oscillation, the motor is moved to the destination position. The midpoint and delay used are an approximation of the ideal values. These result in very good results with a fixed time to move any distance, and a small amount of ringing at the end of the movement. The ringing at the end of the motion does not depend on the amplitude of the motor movement. Rather, it depends on the inaccuracy of the midpoint and delay calculations. A calibrated look-up-table approach would be necessary to eliminate the ringing completely.
4) *Dual two-step.* The two-step method is used to move

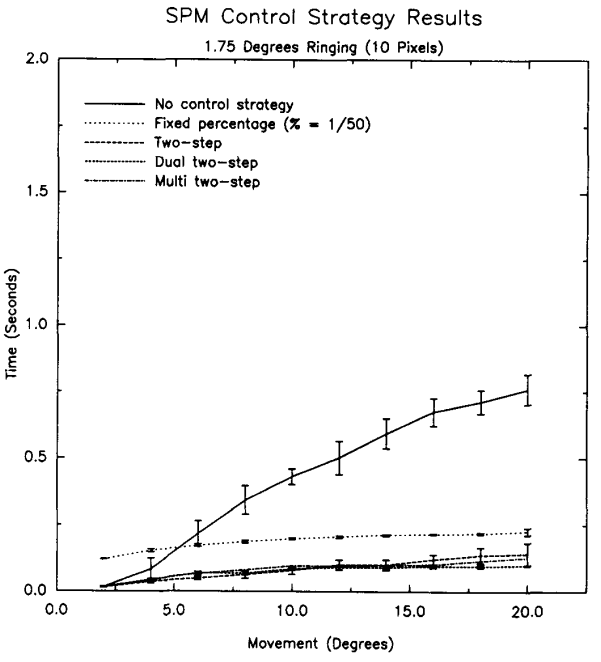

Fig. 12. Results of different open-loop control strategies to reduce the ringing of the SPM. Times reported are those after which amplitude of the ringing has been reduced to 1.75° (10 pixels in our camera). Control strategies are discussed in the text.

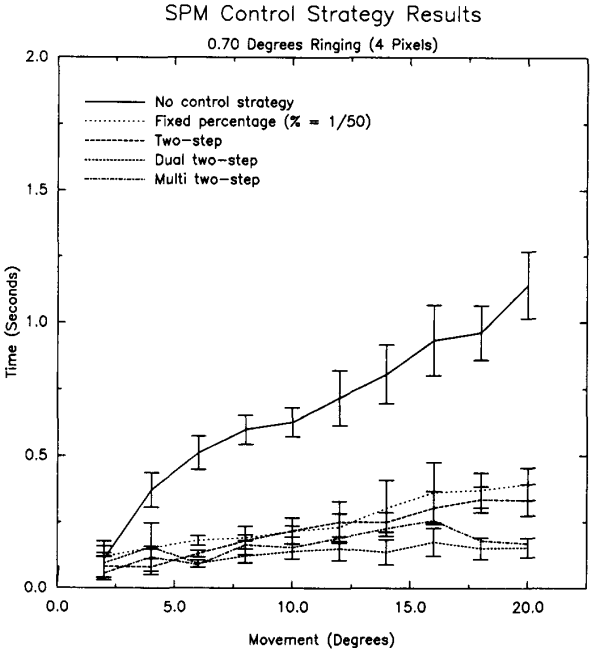

Fig. 13. Results of different open-loop control strategies to reduce the ringing of the SPM. Times reported are those after which amplitude of the ringing has been reduced to 0.70° (4 pixels in our camera).

first to the midpoint, and then to the endpoint. This theoretically takes twice as long as the single two-step method, but actually results in slightly better results.

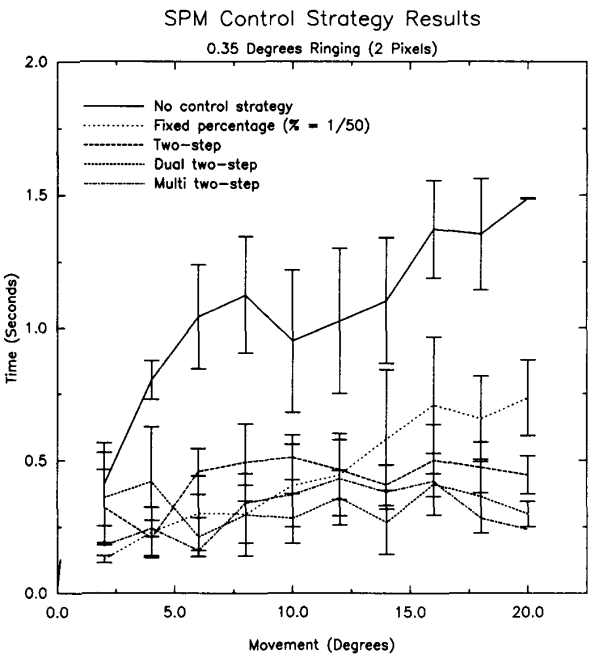

Fig. 14. Results of different open-loop control strategies to reduce the ringing of the SPM. Times reported are those after which amplitude of the ringing has been reduced to 0.35° (2 pixels in our camera).

TABLE I
VELOCITY MEASUREMENTS

Ctrl Method	2° ringing	4° ringing	10° ringing
No control	408/1480	110/1140	18/760
Fixed percentage	127/734	120/395	120/227
Two-step	332/445	83/334	16/143
Dual two-step	359/298	96/155	18/100
Multi two-step	179/240	56/171	17/128

5) *Multiple two-step.* The two-step method is used multiple times, always moving halfway between the current position and the destination position. This theoretically takes time $O(\log(\Phi))$ where Φ is the angular distance between the initial and destination positions. Practically, it produced results very similar to the dual two-step method.

Our measuring apparatus was fairly noisy, resulting in the high variance reported. It is clear that all four control strategies provided substantial improvement over the uncontrolled performance. Of these, the two-step methods are a little better than the fixed percentage approach. Because of the noise in our measurements, it is not clear which two-step method is the best.

The results are summarized in Table I. For each control strategy, the time to move 2 degrees and to move 20 degrees are given for each of three ringing requirements. The times are specified in milliseconds.

It should be stressed that the results from these two-step open-loop control strategies were obtained with approximate calculated values for the mid-point and timing values. We fully expect that with a calibrated look-up-table approach, as with the position calibration of Section V, we will obtain substantially better results.

VIII. Conclusion

We have developed a new miniature pan-tilt actuator suitable for pointing a camera. The spherical pointing motor (SPM) is comparable in capabilities, yet at least an order of magnitude less in size and cost, then other pan-tilt actuators in common use. It is easy to use since it is an absolute positioning device and is run open-loop. A set of currents applied to the coils moves the motor and holds it at a fixed position. Consisting of wire wound around a metal form, a simple gimbal, and a small rare-earth magnet, the SPM is arguably the smallest and least expensive possible device capable of pointing a camera accurately and at high speed.

In this paper, we described the theory, design and use of the SPM. It is shown that the SPM must be designed with the permanent magnets and the optical axis of the camera positioned in a particular orientation with respect to the gimbal. A discussion of the electromagnetic theory of the SPM shows that the accuracy of the motor is dependent on the friction of the bearings, and thus the mechanical design of the SPM is very important. Equations relating the theoretical coil currents to the motor position are derived. These are then used to calibrate the motor to find the precise relation between coil currents and motor position. The dynamics of the motor are then explored and several open-loop control strategies are examined. Finally, we give results measuring the motor repeatability and velocity.

The SPM currently has good enough operating characteristics to be used in active computer vision systems. We expect to improve its capabilities to move at greater speeds with more precision, and to handle larger loads, such as miniature commercial CCD cameras, by calibrating the control strategies and/or adding feedback for closed-loop operation.

References

[1] A. Lynn Abbott and N. Ahuja, "Active surface reconstruction by integrating focus, vergence, stereo, and camera calibration," *International Conference on Computer Vision*, 1990.

[2] P. K. Allen, B. Yoshimi, and A. Timcenko, "Real-time visual servoing," in *Proceedings of the 1991 IEEE International Conf. on Robotcs and Automation*, IEEE Computer Society Press, April 1991, pp. 851–856.

[3] A. A. Baloch and A. M. Waxman, "Behavioral control of the mobile robot mavin," in*Neural Networks: Concepts, Applications, and Implementations, Volume IV*, Antognetti and Milutinov, Eds. Englewood Cliffs, NJ: Prentice Hall, 1991.

[4] B. B. Bederson, "A miniature space-variant active vision system: Cortex-I," Ph.D. thesis, Computer Science Department, GSAS, New York University, 1992.

[5] B. B. Bederson, R. S. Wallace, and E. L. Schwartz, "Calibration of the spherical pointing motor," in *SPIE Conference on Intelligent Robots and Computer Vision*, International Society for Optical Engineering, November 1992.

[6] B. B. Bederson, R. S. Wallace, and E. L. Schwartz, "A miniaturized active vision system," in *11th International Conference on Pattern Recognition*, 1992.

[7] P. J. Burt, "Algorithms and architectures for smart sensing," in *Proc. DARPA Image Understanding Workshop*, pp. 139–153, 1988.

[8] P. J. Burt, "Attention mechanisms for vision in a dynamic world," in *9th IEEE Intl. Conf. on Pattern Recognition*, pp. 977–987, 1988.

[9] C. Brown, Ed. "The Rochester robot," Technical Report 257, University of Rochester, 1988.

[10] J. J. Clark and N. J. Ferrier, "Modal control of an attentive vision system," in *Second Intl. Conf. Computer Vision*, p. 514, 1988.

[11] K. Davey, G. Vachtsevanos, and R. Powers, "The analysis of fields and torques in spherical induction motors," *IEEE Transactions on Magnetics*, vol. 23, no. 1, pp. 273–282, Jan. 1987.

[12] E. D. Dickman and V. Gracle, "Applications of dynamic monocular machine vision," *Machine Vision and Applications*, vol. 1, pp. 241–261, 1988.

[13] A. Foggia *et al.*, "A new three degrees of freedom electromagnetic actuator," in *IEEE Industry Applications Society Annual Meeting*, 1988, pp. 137–141.

[14] E. F. Fichter, "A stewart platform-based manipulator: General theory and practical construction," *The International Journal of Robotics Research*, vol. 5, no. 2, pp. 157–182, 1986.

[15] D. Halliday and R. Resnick, *Fundamentals of Physics, Second Edition, Extended Version*. New York: John Wiley & Sons, 1981.

[16] R. L. Hollis, S. E. Salcudean, and A. P. Allan, "A six-degree-of-freedom magnetically levitated variable compliance fine-motion wrist: design, modeling, control," *IEEE Transactions on Robotics and Automation*, vol. 7, no. 1, pp. 320–332, June 1991.

[17] H. Kawarabayashi, M. Watanabe, Y. Shirai, M. Asade, and J. Miura, "Tracking of a moving object using an active vision system," in *Japan Mechanical Society, Robotics Mechatronics Conference Proceedings*, June 1991, pp. 207–212.

[18] T. Kenjo and S. Nagemori, *Permanent-Magnet and Brushless DC Motors*. Oxford Science Publications, 1985.

[19] E. Krotkov, F. Fuma, and J. Summers, "An agile stereo camera system for flexible image acquisition," *IEEE J. Robotics and Automation*, 4:108–113, 1988.

[20] F. Williams, E. Laithwaite, and G. F. Eastham, "Development and design of spherical induction motors," *Proceedings of the IEEE*, pp. 471–484, Dec. 1959.

[21] K.-M. Lee and C.-K. Kwan, "Design concept development of a spherical stepper for robotic applications," *IEEE Trans. Robotics Automat.*, vol. 7, no. 1, pp. 175–181, Feb. 1991.

[22] D. Raviv and A. Shapira, "Miniature vision-based flight simulator," Technical report, Robotics Center, Florida Atlantic University, 1991.

[23] N. C. Singer and W. P. Seering, "An extension of command shaping methods for controlling residual vibration using frequency sampling," in *Proceedings of the 1992 IEEE International Conference on Robotics and Automat.*, Nice, France, May 1992, pp. 800–805.

[24] N. Stelman, "Design and control of a six-degree-of-freedom platform with variable admittance," Master's thesis, Massachusetts Institute of Technology, Dept. of Mechanical Engineering, 1988.

[25] D. Stewart, "A platform with six degrees of freedom," *Proceedings of the Institution of Mechanical Engineers*, 1965.

[26] R. S. Wallace, "Miniature direct drive rotary actuators," Technical Report TR 634, New York University, CIMS, May 1993.

[27] R. S. Wallace, P.-W. Ong, B. B. Bederson, and E. L. Schwartz, "Space variant image processing," *International Journal of Computer Vision*, vol. 13, no. 1, 1994.

[28] D. Max and R. S. Wallace, "Feedback control for miniature direct drive devices," Technical Report TR 652, New York University, CIMS, November 1993.

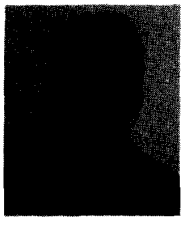

Benjamin B. Bederson, (S'90–M'92), completed the M.S. degree in 1989 and the Ph.D. degree in 1992 at New York University in the Courant Institute of Mathematical Sciences in Computer Science. He graduated with a B.S. from Rensselaer Polytechnic Institute in 1986. From 1990–1992, he was a research scientist at Vision Applications, Inc., performing the work described in this paper. Dr. Bederson is currently a Member of Technical Staff at Bellcore in the Computer Graphics and Interactive Media research group, and a visitor at the New York University Media Research Laboratory. He is currently focusing his research on intuitive user interfaces.

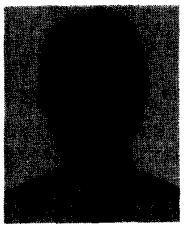

Richard S. Wallace completed his Ph.D. in 1989 and his M.S. in 1986 at Carnegie Mellon School of Computer Science. He graduated with a B.A. from University of Southern California in 1982. From 1986–1989, Wallace was a Member of the Technical Staff, Hughes Research Labs, Malibu, CA. In 1989–1990 he worked as Postdoctoral Fellow at NTT Human Interface Labs, Yokosuka, Japan. Then, from 1990–1992 he was General Manager of Vision Applications, Inc., a research and development firm. Dr. Wallace is now Assistant Professor of Computer Science at the Courant Institute of Mathematical Sciences, New York University. His research interests include robotics, computer vision and pattern recognition.

Eric L. Schwartz, (M'83–M'91), received the Ph.D. degree in high energy physics from Columbia University in 1973, and has served as Associate Professor of Computer Science (Courant Institute of Mathematics) and Psychiatry (New York University Medical Center). He is currently Professor of Cognitive and Neural Systems, Professor of Electrical and Computer Systems and Professor of Anatomy and Neurobiology at Boston University. His research interests include experimental studies of cortical visual architectures in monkeys and humans, and computational modeling of visual anatomy, psychophysics, physiology and function. In 1989, he founded Vision Applications, Inc., where he has served as Chief Research Scientist, and consulted on the design and implementation of miniaturized computer vision systems for performing real-time space-variant active vision. Photograph not available at the time of publication.